Cascaded Fuzzy Logic based Arc Fault Detection in Photovoltaic Applications Summary

Benjamin Grichting, Josef Goette and Marcel Jacomet
Bern University of Applied Sciences, HuCE-microLab
CH-2501 Biel-Bienne, Switzerland

Abstract

Arc faults in photo-voltaic (PV) systems are dangerous events and can create huge damage. If the inverter has the information of an existing arc fault in the system, it can capture counter measures. We present an algorithm which detects such arc faults with only low demands in computation power and resolution.

I. Introduction

In the United States, each year over 20'000 fires are attributed to electrical malfunction. These fires result in 280 deaths each year [1]. Arc faults in a privately installed PV system can cause such a fire. The heating power of an arc can easily emblaze surrounding material. Arc faults occur at critical points, as for example in rusty contacts, in defect modules, or in connector blocks. If mechanical load, like wind, provokes a short interrupt, a constant arc at these critical points can occur. In Switzerland, such fires have already occured at PV Plant Mt Soleil near St-Imier, in 2006 a considerable number of arcs ocurred in defective modules in the PV Plant on the roof of the Bern University of Applied Science. In the last years, also in Germany several fires were reported [2].
So the National Electrical Code (NEC) 2011 [4] dictates an Arc Fault Circuit Interrupter (AFCI) for DC PV systems operating at 80 VDC or higher. We expect that such a law is soon passed also in Europe too, thus all inverters must have a unit to detect arc faults in PV systems. Until now however, only a few systems exhibit such a detector. For inverter manufacturers it is interesting to know, how to combine the existing parts with a new detector. So the algorithm has to be as simple as possible such that it can operate in already existing controllers.
We here present an algorithm that achieves the mentioned goals. It has low computational demands and works with most standard ADC's contained in controllers. It bases on our experiences we made with the measurements described in Section II. With the help of these measurements we made an analysis (Section III) to find some characteristics to develop the final algorithm (Section IV).

II. Proposed Approach

The arc detector must be a part of the inverter. It detects an arc fault in the PV plant. The PV plant is always another system and cannot be easily modeled. Therefore we do not consider methods like impedance spectroscopy because of the high complexity of the complete system. Instead our algorithm bases on measurements of the input signals to the inverter. Figure 1(a) shows the block diagram of the automated measuring setup. The measurement unit is composed of

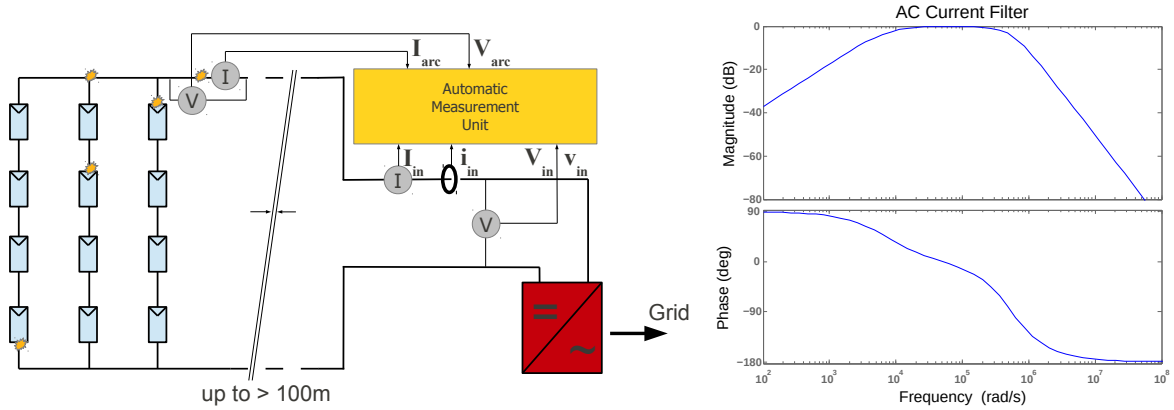

(a) Automatic Measuring System

(b) Bode Plot of AC Current Filter

Fig. 1. The whole measurement system with different arc locations and frequency characteristics.

a Data Acquisition (DAQ) Box NI DAQ USB-6566 controlled by a laptop. We measure 6 channels: $V_{\mathrm{arc}} \mathrel{\hat{=}}$ DC voltage over arc; $I_{\mathrm{arc}} \mathrel{\hat{=}}$ DC current in arc; $I_{\mathrm{in}} \mathrel{\hat{=}}$ DC inverter input current; $V_{\mathrm{in}} \mathrel{\hat{=}}$ DC inverter input voltage; $i_{\mathrm{in}} \mathrel{\hat{=}}$ AC inverter

input current; $v_{\mathrm{in}} \mathrel{\hat{=}}$ AC inverter input voltage. The channel V_{arc} serves as trigger source. If a trigger event occurs, $2.7\,\mathrm{s}$ of all channels with $0.5\,\mathrm{s}$ pre-trigger are recorded with a sampling rate of $2\,\mathrm{MSamples}$ per second and a resolution of $16\,\mathrm{bits}$. The recording time is limited by the buffer size of the DAQ Box, which is in our case $32\,\mathrm{MSamples}$.

A. Front End

The front end is divided into two parts: The first part is mobile and is always coupled with the arc fault generator (see details in II-B) and measures V_{arc} and I_{arc}. We condition the signals with a first order low-pass filter with cutoff-frequency of approximately $1.5\,\mathrm{kHz}$. These signals are not relevant for our algorithm and serve only as trigger sources. The more important second part is near of the inverter. It consists an AC and a DC section. We need DC values to determine the operating point of the inverter. More interesting for us are the AC measurements. The current is measured over a toroidal transformer with subsequently filtering. Figure 1(b) shows the Bode-plot of the i_{in} measurements. We see a bandpass characteristic with corner frequencies at approximately $1\,\mathrm{kHz}$ and $100\,\mathrm{kHz}$. The high-frequency slope is $-40\,\mathrm{dB/DEC}$, so at the Nyquist frequency of $1\,\mathrm{MHz}$ we have already a damping of $40\,\mathrm{dB}$.
The Bode-plot of v_{in} measurements looks the same, since we use for decoupling the high voltage an RC high-pass filter followed by a corresponding low-pass filter of second order.

B. Arc Fault Generator

The norm UL1699B [3] from Underwriter Laboratories (UL)[1] describes how the different arc faults have to be created. The arc fault generator consists of the arc-producing electrodes and a parallel break contact. If the break contact is pressed, the current flows over the electrodes, the steel wool between the predefined electrode distance burns, and a constant electric arc appears between the electrodes. The UL standard dictates a polycarbonate tube around the electrodes containing the steel wool. Because in our measurements in most cases no arc could be produced, we have performed all measurements without this tube.
In addition to the dictated distances of the electrodes, measurements with varying distance have also been done: The current flows over the electrodes and simultaneously the distance becomes larger. The motivation for this method is to prevent a burning of the steel wool which makes it much easier to detected the inception of an arc fault at the input of the inverter.

C. Database

During the first half of 2012, we have built a database with several hundred measurements of arc faults. All measurements have been done in collaboration with the PV Lab of the Bern University of Applied Sciences in Burgdorf.[2] With the help of this database, the measurements can easily be selected by their properties, like input voltage, arc power, distance of the electrodes and the like. Various constellations of arc location, supply, and distances are possible. In the project description on the website of our HuCE microLab, we make available a link to this database.[3]

III. ANALYSIS

A. Frequency Spectrum

Here we analyze the change of the frequency spectrum when an arc fault occurs. We compute the Fast Fourier Transform (FFT) before ($I_{\mathrm{no-arc}}[f]$) and one during ($I_{\mathrm{arc}}[f]$) the arc is burning. To obtain a number describing how large the signal energy is in a given bandwidth, we build the absolute sum in this band.

$$S_{\mathrm{no-arc}} = \sum_{f_{\min}}^{f_{\max}} |I_{\mathrm{no-arc}}[f]| \;, S_{\mathrm{arc}} \sum_{f_{\min}}^{f_{\max}} |I_{\mathrm{arc}}[f]| \tag{1}$$

To scale the relation between S_{arc} and $S_{\mathrm{no-arc}}$ we calculate N according to

$$N = \frac{S_{\mathrm{arc}} - S_{\mathrm{no-arc}}}{S_{\mathrm{arc}} + S_{\mathrm{no-arc}}} \tag{2}$$

to abstain a number between -1 and 1 which represents the change in frequency spectrum when a narc turns on.
We first look at a system consisting a high voltage battery stack as supply and an ohmic load ($8.25\,\Omega$). Since the large input capacity of inverters short-circuits nearly all frequencies, below we refer only to the current spectrum. Figure 2(a) shows this situation. An interesting observation is that the most energy of the arc fault noise is visible in the band from 0 to $10\,\mathrm{kHz}$. We observe this phenomenon in nearly all measurements except for the measurements in the PV Plant in Biel.[4]

[1] See the website `http://www.ul.com`.

[2] See the website `http://www.pvtest.ch`.

[3] `http://microlab.ti.bfh.ch/research/projects/afci-pv-systems/`: Only a preliminary version with limited functionality is online. The final version will be available by 2013.

[4] See our database at `http://microlab.ti.bfh.ch`.

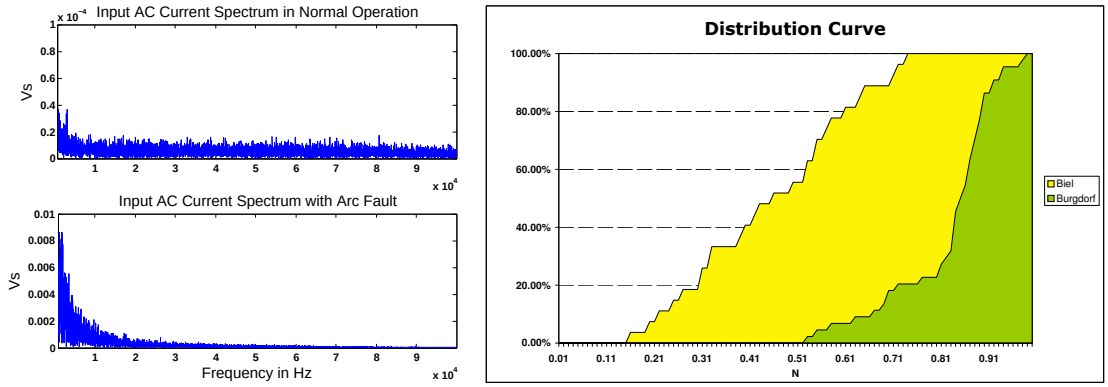

(a) Amplitude density spectrum with battery as supply (b) Cumulated distribution function of N for two PV plants ($f_{\min} = 0\,\text{kHz}$, $f_{\max} = 10\,\text{kHz}$

Fig. 2. Signal energy change—take care of the different scales—and our measure N for measurements in different PV plants.

Figure 2(b) illustrates the cumulative distribution function of N for two different PV plants. One plant is located in Burgdorf on the roof of the Bern University of Applied Sciences building, and the other is the test plant from Sputnik Engineering in Biel, next to a railroad. The situation for this second plant looks not very nice. The native noise in this plant is much higher than in other ones. The calculated measure N is for the frequency band up to $10\,\text{kHz}$ nearly uniformly distributed. But the goal of our measure is to set a threshold at a defined level with all values above it being detected as arc fault. A possibility to improve the situation would be to increase the bandwidth, but it shows also that only supervising the spectrum is insufficient. We need some more indicators.

B. Peak Detection

We further have observed in all measurements at the beginning of an arc fault a clearly visible peak in i_{in}. Interesting is the difference in the peak shape; in the arc faults provoked as dictated in the UL standard, the burning of the steel wool is clearly visible. In our generated cases with growing electrode distances, the peak has much less noise.

C. Operating Point

An appearing arc fault in the system abruptly changes input power to the inverter. Fluctuations in irradiation of the sun are not as fast. However, we must distinguish between large and small plants. The case of an arc burning with $40\,\text{W}$ in a MW plant is not easy to detect at the inverter input. The abrupt change of the operating point can, however be used to prevent faulty activation. For instance if some switching operation is running, power changes over $100\,\%$ are possible. Such a decrease/increase in power is probably (hopefully) not be provoked by an arc fault.

IV. Detection Algorithm

Out detection algorithm bases on the above three indicators. So we must convert them into a form that a controller easily handles.

A. Segmentation

Because we target a real time application, the signal has to be analyzed on the level of received samples. The algorithm calculates three different kind of segments. A segment is a property of the signal in a given interval. The different segments correspond to the three indicators found in the previous section III. There you have 'Frequency Spectrum', 'Peak Detection' and 'Operating Point'. The corresponding segments are 'Signal Energy', 'Peak' and 'DC Power'. Figure 3(a) illustrates these segmentations. On the top the input signal i_{in} is modeled. The more red the signal is the more noise it contains.

1) Signal Energy: In Section III we have determined the signal energy in the $10\,\text{kHz}$ band via FFT. However the computation effort is to large for a controller. Therefore, we low-pass filter the signal and then compute an approximation for the energy

$$E_x \approx \sum_{a}^{b} |i_{\text{in}}[k]|^2 \,, \tag{3}$$

where the variables a and b are the borders of the segment and x is the segment number.

2) DC Power: The Segment P_x contains the input power to the inverter in the given time interval. This value can be calculated with I_{in} and V_{in}.

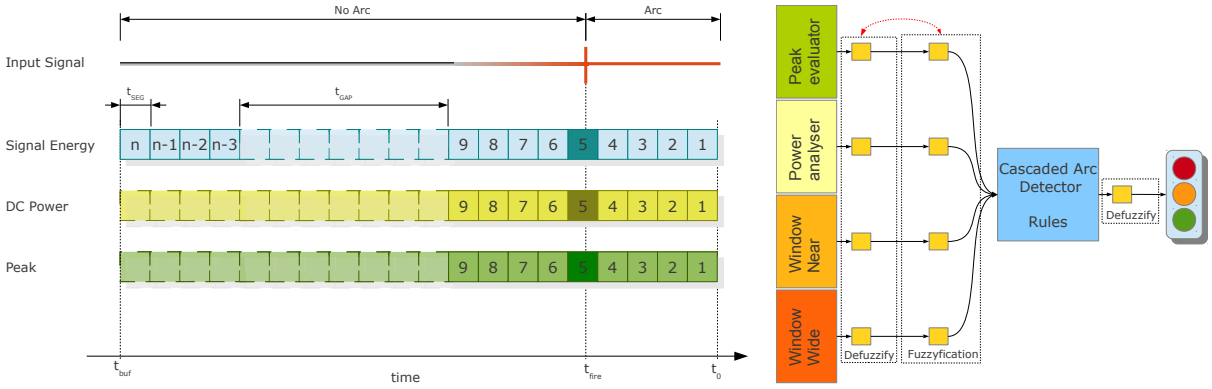

(a) Segmentation of input variables (b) Cascaded fuzzy detection

Fig. 3. Overview over input variables (segments) for our algorithm and the modular fuzzy logic detection.

3) Peak: The measure of the peak size is calculated using the standard deviation of i_{in}. When we assume that the mean value of i_{in} is 0, then the standard deviation can be approximately calculated with the help of E_x:

$$\sigma_x \approx \sqrt{\frac{1}{b-a} \cdot \sum_{a}^{b} \left(i_{\text{in}}[k]\right)^2} = \sqrt{\frac{1}{b-a} \cdot E_x}. \tag{4}$$

We may define a threshold a $\tau_x = m \cdot 3 \cdot \sigma_x$ where m is an adjustable parameter. So the peak size in the particular segment can be determined in a manner similar to the measure in (2).

$$PK_x = \frac{\max\left(|i_{\text{in}}[k]|\right)_{k=a}^{k=b} - \tau_x}{\max\left(|i_{\text{in}}[k]|\right)_{k=a}^{k=b} + \tau_x} \tag{5}$$

B. Cascaded Fuzzy Detection

We detect changes in either the signal energy, or the operating point, or the peaks can be detected via different primary fuzzy detectors. The algorithm uses four different primary fuzzy detectors:

1) Peakevaluator: Evaluates the peak size. Inputs are the peak size segment PK_5 and relations of the signal energy segments $E_{3\ldots7}$. The peak is identified as `large`, when it is in the interval of segment 5. So the algorithm has enough data to compare the segments before and after the peak.

2) Window Near: Compares the signal energy before and after the peak similar to (2).

3) Window Wide: If an arc is burning not immediately with its full power, the *Window Near* detector has no chance to detect a growth in the noise energy. So the *Window Wide* detector supervises the changes of noise in a wider time interval.

4) Poweranalyser: Observes continuously the input power to the inverter. In most cases of arc faults, the power does not change too much. So this detector serves mainly to prevent faulty activation.

The outputs of these four detectors are inputs for the master fuzzy detector, see figure 3(b). The advantage of such a system is that it can be improved on the run due to its modularity. The presently used prototype of our Arc Fault Detector seconds all critical events, allowing to modify rules and/or to add new rules.

V. Results

Experiments in the laboratory show that 100 % of the arc faults, with a given distance of the electrode, can be detected. The algorithms detects all synthetic arc faults of the database with an output value larger than 0.8.

VI. Acknowledgment

We like to thank to Sputnik Engineering AG, especially Joerg Marzoner and Norman Bayer for their assistance and for providing different inverters. Furthermore we want to thank to the PV Lab in Burgdorf, especially Daniel Gfeller for the measurements, and Prof. Heinrich Haeberlin and Prof. Urs Muntwyler for their support; and Marcel Jost and Prof. Roger Weber from the Institute for Mobile Communications, research group embedded systems, for the future implementation.

References

[1] U.S. Fire Administrations (USFAs) National Fire Incident Reporting System, December 2011.
[2] H. Haeberlin, Arc Detector as an External Accessory Device for PV Inverters for Remote Detection of Dangerous Arcs on the DC Side of PV Plants, World Conference on Photovoltaic Energy Conversion, Valencia, Spain, 2010.
[3] Standard UL1699B - PHOTOVOLTAIC (PV) DC ARC-FAULT CIRCUIT PROTECTION, Underwriter Laboratories, http://www.ul.com.
[4] National Electrical Code 2011., NFPA, ISBN 978-087765914-3, 690.11 Arc-Fault Circuit Protection (Direct Current), p. 70-599.